

## Young's modulus reduction of defective nanotubes

Nicola M. Pugno<sup>a)</sup>

Department of Structural Engineering and Geotechnics, Politecnico di Torino, Corso Duca Degli Abruzzi 24, 10129 Torino, Italy

(Received 6 October 2006; accepted 30 November 2006; published online 22 January 2007)

In this letter the author calculate, by applying fracture mechanics, Young's modulus reduction for a nanotube, imposed by the presence of nanodefects, with specified size, shape, and number. The results are compared with atomistic and continuum simulations. Vacancy fraction, eccentricity, orientation, and interaction of defects are found to be the key parameters influencing the stiffness degradation. © 2007 American Institute of Physics. [DOI: 10.1063/1.2425048]

Carbon nanotubes (CNTs) have extremely high axial Young's modulus, about 1 TPa.<sup>1-6</sup> This outstanding elastic stiffness holds for nearly perfect CNTs. However, if CNTs are defective, one can expect that even a small number of defects in their atomic network will result in some degradation of their characteristics, as recently emphasized analytically for mechanical strength.<sup>7-10</sup> Even if Young's modulus reduction is expected to be less critical than the related and tremendous strength reduction [just a single vacancy reduces the strength of an isolated small nanotube by a factor of about 20% (see Refs. 7 and 8)], such an elastic degradation cannot be neglected and has to be accurately predicted for high-nanotechnology applications. For example, whereas the presence of a defect could become critical for the ultimate strength of the carbon-nanotube-based space elevator megacable<sup>10</sup> (see also the related Ref. 11), it could destabilize the cable orbit.<sup>12</sup> Such reasons have motivated the present study.

Consider a single nanotube having thickness  $t$ , radius  $r$ , and length  $l$ , under a tension  $\sigma$  (or force  $F=2\pi r t \sigma$ ) and containing a nanocrack of length  $2a$  orthogonal to the applied load. The variation of the total potential energy induced by the presence of the crack is  $\Delta W = \Delta L - F\Delta\delta$ , where  $L$  is the elastic energy stored in the nanotube and  $\delta = F/S$  is the elastic displacement;  $S$  is thus the nanotube stiffness, i.e.,  $S = 2\pi r t E/l$ , with  $E$  as Young's modulus. Applying Clapeyron's theorem,<sup>13</sup>  $\Delta L = \frac{1}{2}F\Delta\delta$  and consequently  $\Delta W = \frac{1}{2}F^2/S^2\Delta S$ . The same result can be deduced for imposed displacement rather than imposed force. Furthermore, according to fracture mechanics,  $dW = -GdA$ , where  $A$  is the crack surface area, i.e.,  $2at$ , and  $G$  is the energy release rate (the crack will propagate when  $G$  reaches a critical value  $G_C$ , the so-called material fracture energy, per unit area created). The energy release rate is related to the stress-intensity factor  $K$  at the tip of the crack, reported for hundreds of different configurations in the stress-intensity factor handbooks, via Irwin's correlation,<sup>13</sup>  $G = K^2/E$ . Let us consider the presence of an isolated crack and neglect the energy associated with the nanotube circumferential curvature as well as the crack tip self-interactions: accordingly,  $K = \sigma\sqrt{\pi a}$  since this case is analogous to the well-known Griffith case.<sup>13</sup> Consequently, equating the two expressions for  $\Delta W$ , i.e.,  $\frac{1}{2}F^2/S^2\Delta S = -2t\int_0^a G(a)da$ , we deduce the variation of Young's modulus, imposed by the presence of a crack of half-length  $a$  (sub-

script  $a$ ) with respect to its theoretical (subscript th, i.e., defect-free) value, in the following simple form:  $E_a/E_{th} = 1 - a^2/(rl)$ . We assume the presence of an additional transversal crack of half-length  $b$ , noninteracting with the previous one. According to our previous result,  $E_{a\oplus b}/E_a = 1 - b^2/(rl) \equiv E_b/E_{th}$ , where  $E_{a\oplus b} \equiv E_{b\oplus a}$  denotes Young's modulus of the nanotube containing the two noninteracting transversal cracks. Thus, by multiplying the two previous results, we derive  $E_{a\oplus b}/E_{th} = (E_a/E_{th})(E_b/E_{th}) = (1 - a^2/(rl))(1 - b^2/(rl))$ .

For different schemes, e.g., interacting cracks, the previous approach remains valid if  $K = \sigma\sqrt{\pi a}$  is substituted with the corresponding value of the stress-intensity factor (from the stress-intensity factor handbooks). However, to have an idea of the possible role of the interaction we note that it will be maximal for collinear coalescing cracks. After coalescence,  $E_{a+b}/E_{th} = 1 - (a+b)^2/rl$ , the interaction is predicted to be  $I_{max} = (E_{a\oplus b} - E_{a+b})/E_{th} = (a^2b^2 + 2abrl)/(rl)^2 \approx 2ab/(rl)$ , where the last approximation is valid only for small crack lengths (with respect to  $r$  and  $l$ ).

We are now ready to derive a general law. Let us consider  $N$  cracks having size  $a_i$  or, equivalently,  $M$  different cracks with multiplicity  $N_i$  ( $N = \sum_{i=1}^M N_i$ ). Noting that  $n_i = 2a_i/q$  represents the number of adjacent vacancies in a crack of half-length  $a_i$ , with  $q$  atomic size, and  $f_i = N_i n_i / (2\pi r l / q^2)$  its related numerical (or volumetric) vacancy fraction, we can write (the approximations are valid for small cracks)

$$\begin{aligned} \frac{E}{E_{th}} &= \prod_{i=1}^N \frac{E_{a_i}}{E_{th}} = \prod_{i=1}^N \left( 1 - \frac{a_i^2}{rl} \right) = \prod_{i=1}^M \left( 1 - \frac{a_i^2}{rl} \right)^{N_i} \\ &\approx 1 - \sum_{i=1}^M \frac{N_i a_i^2}{rl} = 1 - \sum_{i=1}^M \alpha_i f_i n_i, \end{aligned} \quad (1)$$

with  $\alpha_i = \alpha \equiv \pi/2$ . Extending the interpretation of our formalism, we note that  $n_i = 1$  would describe a single vacancy, i.e., a small hole. Thus, different defect geometries, from cracks to circular holes, e.g., elliptical holes, could in principle be treated as a first approximation by Eq. (1), interpreting  $n_i$  as the ratio between the transversal and longitudinal (parallel to the load) defect sizes. Thus, introducing the defect eccentricity  $e_i$  as the ratio between the lengths of the longer and shorter axes for the  $i$ th defect, we must have  $n_i(\beta_i) \approx e_i \sin^2 \beta_i + 1/e_i \cos^2 \beta_i$ , where  $\beta_i$  denotes the angle between the longer axis and the uniaxial load. Furthermore, considering  $N=2$  coalescing identical cracks of half-length  $a$ ,

<sup>a)</sup>Electronic mail: nicola.pugno@polito.it

TABLE I. Comparison between the present theory (theor) and the atomistic simulations (num) reported in Ref. 14. The constants  $k_i$  governing the elastic reduction ( $E_{th}/E \approx 1 + k_1 c_1 + k_2 c_2 + k_3 c_3$ ) calculated according to the present theory ( $k_i = \alpha_i n_i^2 q^2 / (2\pi r)$ ) are compared with those derived for the  $(m, p)$  nanotubes numerically investigated in (Ref. 14), considering defects with reconstructed (a) and nonreconstructed (b) vacancies; two different nonreconstructed orientations ( $b1, b2$ ) for two and three atoms missing were numerically investigated, (see Ref. 14, for details). All the reported quantities are in angstrom. Parameters used are  $\alpha_i = \pi/2$ ,  $n_i = i = 1, 2, 3$ ,  $r \approx 0.0392\sqrt{m^2 + p^2 + mp}$ , and  $q \approx 0.246$  nm (Ref. 7).

$(m, p)$	$r$	$k_1^{(theor)}$	$k_1^{(num)}$	$k_2^{(theor)}$	$k_2^{(num)}$	$k_3^{(theor)}$	$k_3^{(num)}$
(5,5)	3.39	0.45	1.2 <sup>(a)</sup> 1.2 <sup>(b)</sup>	1.79	1.4 <sup>(a)</sup> 1.7 <sup>(b1)</sup> 2.8 <sup>(b2)</sup>	4.02	1.8 <sup>(a)</sup> 2.2 <sup>(b1)</sup> 3.6 <sup>(b2)</sup>
(9,0)	3.53	0.43	1.1 <sup>(a)</sup> 1.1 <sup>(b)</sup>	1.71	1.2 <sup>(a)</sup> 1.3 <sup>(b1)</sup> 2.1 <sup>(b2)</sup>	3.86	1.6 <sup>(a)</sup> 2.4 <sup>(b1)</sup> 3.6 <sup>(b2)</sup>
(10,10)	6.79	0.22	0.8 <sup>(a)</sup> 0.5 <sup>(b)</sup>	0.89	1.0 <sup>(a)</sup> 0.7 <sup>(b1)</sup> 1.3 <sup>(b2)</sup>	2.01	1.2 <sup>(a)</sup> 1.0 <sup>(b1)</sup> 1.5 <sup>(b2)</sup>
(17,0)	6.67	0.23	0.8 <sup>(a)</sup> 0.5 <sup>(b)</sup>	0.91	1.0 <sup>(a)</sup> 0.7 <sup>(b1)</sup> 1.0 <sup>(b2)</sup>	2.04	1.2 <sup>(a)</sup> 1.2 <sup>(b1)</sup> 1.7 <sup>(b2)</sup>

noting that the maximum interaction would be  $I_{max} > 2a^2/(rl)$  we deduce for such a case  $\alpha_{max} > \pi$ . Thus, different  $\alpha_i$  allow one to describe defect-defect or defect-boundary or self-defect (tip) interactions and a reference value could be considered,  $\alpha \approx \pi$  ( $I_{max} \approx 2a^2/(rl)$ ).

If only one defect typology (e.g., a crack composed by  $n$  adjacent vacancies) is present with a fraction  $f$  in a nanotube or nanotube bundle, the related Young modulus  $E(f, n)$  must satisfy

$$\frac{E(f, n)}{E_{th}} \approx 1 - \alpha f n, \quad (2)$$

with  $n(\beta) \approx e \sin^2 \beta + 1/e \cos^2 \beta$  and  $\alpha \geq \pi/2$ .

We note that our treatment can be viewed as a generalization of the interesting approach proposed in Ref. 14, being able to quantify the constants  $k_i$  fitted by atomistic simulations in Ref. 14 for three different types of defect. In particular, rearranging Eq. (1) and in the limit of three small cracks, we deduce  $E_{th}/E \approx 1 + k_1 c_1 + k_2 c_2 + k_3 c_3$ , identical to their Eq. (15), in which  $c_i = N_i/l$  is the linear defect concentration and  $k_i = \alpha_i n_i^2 q^2 / (2\pi r)$ . These authors<sup>14</sup> consider one, two, and three atoms missing, with and without reconstructed bonds; for nonreconstructed bonds two alternative defect orientations were investigated for two and three atoms missing (for details see Ref. 14). Even if their defect geometries are much more complex than the nanocracks that we consider here, the comparison between our approach and their atomistic simulations, which does not involve best-fit parameters, shows a good agreement, as summarized in Table I.

Now let us compare the results of Eq. (2) with the three dimensional atomistic and continuum simulations on extension behavior of single crystals containing nanoholes reported in the relevant paper in Ref. 15. A rectangular plate with width  $W=100q$  and height  $H=200q$  ( $q$  is the triangular

lattice constant, 0.2892 nm for the investigated fcc Ag) containing a circular hole was stretched along the “vertical” direction, see Fig. 1 (left). Twelve different hole radii  $R$ , varying from  $5q$  to  $40q$ , were investigated with both finite element methods (FEMs) or molecular dynamics (MD) simulations. The related defect-free structures were also investigated to derive the theoretical Young modulus. FEM Young modulus reductions were found to be comparable to those predicted by MD simulations, even if, in general, slightly larger. According to Eq. (2), we expect  $E(R)/E_{th} \approx 1 - k(R/q)^2$ , with  $k = \alpha \pi q^2 / (WH) \approx 5.0 \times 10^{-4}$  for  $\alpha = \pi$ . We note that these authors fitted their 26 simulations using exactly the previous equation (see their Fig. 7) and, remarkably, with  $k_{fit} \approx 4.4 \times 10^{-4}$  (or  $\alpha_{fit} \approx 2.76$ ), in strong agreement with our prediction.

We further compare Eq. (2) with two additional sets of four simulations each [(a–d), (e–h)],<sup>15</sup> performed maintaining the volumetric fractions constant (0.063 and 0.014), see Fig. 1 (right): (a) one single hole of radius  $20q$  and two (b) horizontal or (c) vertical holes of radius  $14.14q$  (at distance  $\sim 3R$ ), (d) four holes of radius  $10q$  placed at the vertic of a square (with size  $\sim 4R$ ), and (e) one circular hole of radius  $9.54q$  and one elliptical hole with long and short axes of  $20q$  and  $4.5q$ , respectively, (f) horizontal, (g) vertical, or (h) inclined by an angle of  $\pi/4$ . The comparison is summarized in Table II and again shows a good agreement.

We conclude that our approach, summarized by Eqs. (1) and (2), could have interesting high-nanotechnology applications; it quantifies the role of nanodefects on elasticity of single crystals, such as carbon nanotubes. The reported three comparisons with atomistic and continuum simulations confirm the reliability of our approach. Clearly, the trivial prediction purely based on the volumetric fraction, i.e.,  $E/E_{th} \approx 1 - f$ , has to be considered wrong in the light of Eq. (2):

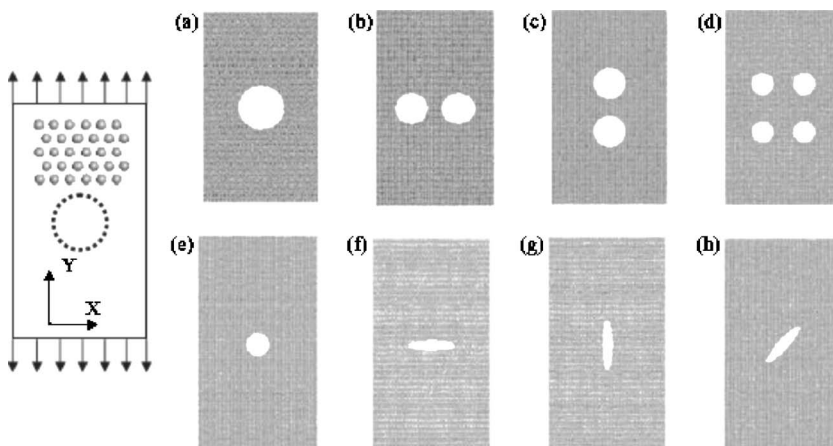


FIG. 1. Geometries numerically investigated in Ref. 15 (from which the figure has been adapted) and compared with our theory in Table II.

TABLE II. Elasticity of a perforated plate of size of  $100q \times 200q$  (see Fig. 1) with (a) one single hole of radius  $20q$  and two (b) horizontal or (c) vertical holes of radius  $14.14q$  (at distance  $\sim 3R$ ), (d) four holes of radius  $10q$  placed at the vertices of a square (with size  $\sim 4R$ ), and (e) one circular hole of radius  $9.54q$  and one elliptical hole with long and short axes of  $20q$  and  $4.5q$ , respectively, (f), horizontal (g), vertical or (h) inclined by an angle of  $\beta = \pi/4$ . Comparison between MD atomistic simulations, FEM (Ref. 15), and present approach (Theory). The numbers between brackets represent the values of  $\alpha$  needed to identically recover the numerical simulations. Note the higher values observed in the (b) (stronger hole interaction) than in the (c) simulations. All the values are found to be larger than  $\pi/2$  and of the order of  $\pi$  (with the exception of the FEM (g) simulation). The last row simply considers Eq. (2) with  $\alpha = \pi$ .

$E/E_{th}, (\alpha_{fit})$	a	b	c	d	e	f	g	h
MD	0.791 (3.326)	0.779 (3.518)	0.855 (2.31)	0.832 (2.67)	0.953 (3.29)	0.843 (2.47)	0.985 (4.66)	0.917 (2.49)
FEM	0.787 (3.390)	0.760 (3.82)	0.831 (2.69)	0.802 (3.15)	0.936 (4.48)	0.830 (2.68)	0.965 (10.88)	0.901 (2.97)
Theory	0.803	0.803	0.803	0.803	0.955	0.800	0.990	0.895

defects perpendicular to the load with large eccentricity (and/or interaction), even if in small fractional amount, could significantly reduce the elastic properties of a crystal.

The author thanks the support by the Italian Ministry of University and Research (MIUR) and Dorothy Hesson for the final supervision of the English grammar.

<sup>1</sup>M. M. J. Treacy, T. W. Ebbesen, and J. M. Gibson, *Nature (London)* **381**, 678 (1996).

<sup>2</sup>E. W. Wong, P. E. Sheehan, and C. M. Lieber, *Science* **277**, 1971 (1997).

<sup>3</sup>P. Poncharal, Z. L. Wang, D. Ugarte, and W. A. de Heer, *Science* **283**, 1513 (1999).

<sup>4</sup>A. Krishnan, E. Dujardin, T. W. Ebbesen, P. N. Yianilos, and M. M. J. Treacy, *Phys. Rev. B* **58**, 14013 (1998).

<sup>5</sup>J. P. Lu, *Phys. Rev. Lett.* **79**, 1297 (1997).

<sup>6</sup>E. Hernández, C. Goze, P. Bernier, and A. Rubio, *Phys. Rev. Lett.* **80**, 4502 (1998).

<sup>7</sup>N. Pugno and R. Ruoff, *Philos. Mag.* **84**, 2829 (2004).

<sup>8</sup>N. Pugno, *Int. J. Fract.* **140**, 158 (2006).

<sup>9</sup>N. Pugno, *Int. J. Fract.* **141**, 311 (2006).

<sup>10</sup>N. Pugno, *J. Phys.: Condens. Matter* **18**, S1971 (2006).

<sup>11</sup>J. Palmer, *news@nature.com*, 2006.

<sup>12</sup>N. Pugno, H. Troger, A. Steindl, and M. Schwarzbart, *Proceedings of the 57th International Astronautical Congress*, 2–6 October 2007, Valencia, Spain (CD-ROM).

<sup>13</sup>A. Carpinteri, *Structural Mechanics: A Unified Approach* (Taylor & Francis, London, 1997), p. 673.

<sup>14</sup>M. Sammalkorpi, A. Krashennikov, A. Kuronen, K. Nordlund, and K. Kaski, *Phys. Rev. B* **70**, 245416 (2004).

<sup>15</sup>H. A. Wu, G. R. Liu, and J. S. Wang, *Modell. Simul. Mater. Sci. Eng.* **12**, 225 (2004).